Solid/Liquid Phase Change in Presence of Natural Convection: A Thermal Energy Storage Case Study

M. Pinelli*

S. Piva

Dipartimento di Ingegneria—University of Ferrara
Via Saragat, 1-44100 Ferrara, Italy

Solid/liquid phase change process has received great attention for its capability to obtain high energy storage efficiency. In order to analyze these systems, undergoing a solid/liquid phase change, in many situations the heat transfer process can be considered conduction-dominated. However, in the past years, it has been shown that natural convection in the liquid phase can significantly influence the phase change process in terms of temperature distributions, interface displacement and energy storage. In this paper, a procedure to analyze systems undergoing liquid/solid phase change in presence of natural convection in the liquid phase based on the utilisation of a commercial computer code (FLUENT), has been developed. This procedure is applied to the study of a cylinder cavity heated from above and filled with a phase change material. It was found that when the coupling with the environment, even if small, is considered, natural convection in the liquid phase occurs. The numerical results are then compared with available experimental data. The analysis shows that the agreement between numerical and experimental results is significantly improved when the results are obtained considering the presence of circulation in the liquid phase instead of considering the process only conduction-dominated. Furthermore, some interesting features of the flow field are presented and discussed.
[DOI: 10.1115/1.1591204]

Introduction

Thermal Energy Storage (TES) has received increasing attention over the last years, both in civil and industrial applications. In particular, TES systems are becoming to be widely used in combined cycle power plants and gas turbine cogeneration plants, since they can fulfil to various tasks, such as: (i) storing of thermal energy recovered from the hot exhaust stream of the gas turbine to meet daily variations in electrical and energy demand; (ii) ice generation and storage using electrically driven or absorption chillers, for both air conditioning peak shaving and turbine inlet air cooling systems. In all these applications, the use of TES systems has proven to be cost effective, can lower energy costs and utility bills, and, further, reduce maintenance costs [1,2].

A widely used class of energy storage media are the so-called Phase Change Materials (PCMs). These media, characterized by a high value of latent heat per unit mass, seem to offer the best performance in thermal energy storage, due to their capability of absorbing or releasing high rates of energy. Furthermore, PCMs are used in many other applications, as, for instance, in thermal control systems to reduce temperature oscillations [3] or, in space application, in storage units for power production using closed Brayton Cycle [4]. Some of the most widely used PCMs are water, eutectic salts and paraffins.

The interest shown in this process has suggested, in addition to experimental tests, the development of methodologies for the modelling of the phase change phenomenon. The theoretical analysis of problems involving melting or solidification is particularly difficult. In fact, during the solid-liquid phase change, the interface between the two phases moves through the medium and its position is a priori not known. This fact introduces a nonlinearity into the mathematical model which is very difficult to deal with, especially in two- or three-dimensional problems. Moreover, if other factors increase the complexity of the problem, such as variation of material properties and/or boundary conditions variable with arbitrary laws, the solution can become even more difficult.

For all these reasons, only a few one-dimensional analytical solutions exist [5]. In the case of two-dimensional problems, some analytical or approximate methods have been developed for a few specific cases; exhaustive reviews can be found, for example, in [6] and [7].

For more complex processes, always involving melting and/or solidification, only numerical methods offer the possibility of finding a solution. Furthermore, a numerical simulation can provide useful information on some parameters otherwise difficult to be investigated, such as the amount and the evolution in time of stored energy.

In past years, a wide number of numerical methods has been developed (exhaustive reviews can be found in [7–9]) and, in many cases, the codes developed have given good results when applied to real systems. Due to the great difficulties in the solution of the phase change process, these numerical codes have generally been tailored to solve only a particular class of problem. From an industrial point of view, this represents a marked limitation.

In recent years a growing interest in PCM energy storage processes for industrial application has emerged, since their applicability is beginning to become economically affordable. The design of these PCM energy storage systems and the optimization of their performances can be aided through numerical simulations. Meeting these requirements, the commercial CFD codes have included dealing with problems involving a solid/liquid phase change, but it is still very complicated to get a fully convergent solution. In addition, although the phase change models in commercial software should be as general as possible, in reality they can solve reasonably well only some particular problems, such as, for in-

*Corresponding author. Tel.: +39-0532-974889; fax: +39-0532-974870. E-mail address: mpinelli@ing.unife.it
Contributed by the Advanced Energy Systems Division for publication in the JOURNAL OF ENERGY RESOURCES TECHNOLOGY. Manuscript received at the AES Division revised manuscript received May 2001. Associate editor: S. M. Aceves.

stance, solidification of metal ingots. Therefore, it is advisable that these CFD codes should extend their range of applicability to become really industrially attractive.

The above discussion emphasises the importance of developing methodologies that permit the setting up and validation of these codes before their utilisation to solve practical cases. Once these methodologies have been stated, commercial codes can represent a powerful tool. In fact, they are usually easy-to-use, take into account phenomenon, often neglected to simplify the problem but always present in real devices, such as natural convection in the liquid phase, and allow for the simulation of complex three dimensional geometry.

In particular, it has been demonstrated by many authors (see for instance [10] and [11]) that natural convection in the melt can have a significant influence on the heat transfer process in terms of temperature distribution and interface displacement; neglecting its effects, the reliability of the stored energy determination can be significantly altered.

In a previous paper, Casano et al. [12] investigated experimentally a horizontal layer of 99% pure *n*-octadecane heated from above, obtained inside a cylinder cavity of low aspect ratio. The authors used a conduction-based one-dimensional approach, finding appreciable quantitative differences between experimental data and numerical results. Pinelli et al. [13] included the thermal coupling with the environment, but they still considered the process dominated by conduction. Although they found a better agreement between experimental data and numerical results in comparison with the one-dimensional approach used in [12], the improvement was quantitatively small and they suggested incorporation within the model of natural circulation in the liquid phase. This natural circulation was originally not expected to appear during the experiment, since the cavity, laterally insulated and heated from above, was conceived to be one-dimensional and the liquid inside unconditionally stable. In reality, the coupling with the environment, even if small, is certainly present. Hence lateral heat fluxes, whether positive or negative, are present, establishing a temperature difference between the core of the cavity and the lateral boundary and thus, a fluid motion can originate.

In the present work, the same cylinder specimen of [12] and [13] has been studied numerically by means of the commercial code FLUENT [14] in order to establish the role of natural convection and its influence on the heat transfer process. The code performance was previously evaluated with two test cases. In these applications, a solution strategy to obtain convergent and accurate solutions was developed. Then, the particular problem under investigation was solved and the numerical results have been compared with the available experimental data.

Problem Formulation

The problem under investigation refers to an experimental test reported in [12,13]. In Fig. 1, a scheme of the problem geometry and boundary conditions is reported. A cylinder cavity, filled of *n*-octadecane initially at the solid state, is melted from above by a heater, kept at a temperature higher than the phase change temperature, and placed on the top surface of the cylinder. The bottom surface is kept at a temperature lower than the melting point of the test material by a cooling system. The cylinder side surface is surrounded by a thick layer of expanded polystyrene to minimize the coupling with the environment. In this manner, the geometry and the boundary conditions of the experiment were chosen to reproduce at best a one-dimensional problem.

For the mathematical description of the phase change process, the following assumptions are made: (1) the PCM is homogenous, isotropic, and, when liquid, Newtonian and incompressible; (2) the fluid flow in the liquid phase is laminar; (3) the Boussinesq assumption is valid for natural circulation, that is, the density variations are considered only for their contribution to buoyancy, otherwise they are neglected; (4) the phase change takes place at a well defined temperature, namely T_f.

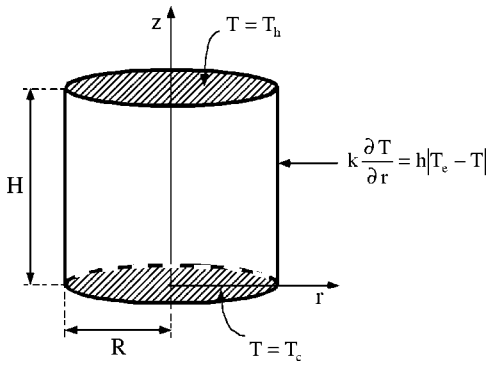

Fig. 1 Geometry and boundary conditions for the problem considered

For the numerical solution of the phase change, the enthalpy-porosity model developed by Voeller and Prakash [15], which is implemented in FLUENT, is used. In this model, the entire domain is considered as a porous medium where the porosity, λ, takes the value $\lambda=1$ in the liquid phase, $\lambda=0$ in the solid phase and $0<\lambda<1$ in the transition region between solid and liquid. Thus, the governing equations are written in terms of a velocity defined as

$$\mathbf{u}=\lambda\mathbf{u}_1 \tag{1}$$

where $\mathbf{u}_1$ is the actual fluid velocity.

Based on the above assumptions and following the enthalpy-porosity model, in two-dimensional axysimmetric co-ordinates the conservation equations are:

Mass

$$\frac{\partial(\rho \mathrm{ru})}{\partial \mathrm{z}}+\frac{\partial(\rho \mathrm{rv})}{\partial \mathrm{r}}=0 \tag{2}$$

Radial momentum

$$\frac{\partial}{\partial \mathrm{t}}(\rho \mathrm{u})+\frac{1}{\mathrm{r}}\mathrm{div}(\mathrm{r}\rho\mathbf{u}\mathrm{u})=\frac{1}{\mathrm{r}}\mathrm{div}(\mathrm{r}\mu\ \mathrm{grad}\,\mathrm{u})-\frac{\partial \mathrm{p}}{\partial \mathrm{r}}+\mathrm{Au} \tag{3}$$

Axial momentum

$$\frac{\partial}{\partial \mathrm{t}}(\rho \mathrm{v})+\frac{1}{\mathrm{r}}\mathrm{div}(\mathrm{r}\rho\mathbf{u}\mathrm{v})=\frac{1}{\mathrm{r}}\mathrm{div}(\mathrm{r}\mu\ \mathrm{grad}\,\mathrm{v})-\frac{\partial \mathrm{p}}{\partial \mathrm{z}}-\rho \mathrm{g}\beta(\mathrm{T}-\mathrm{T}_{\mathrm{ref}})+\mathrm{Av} \tag{4}$$

Energy

$$\frac{\partial}{\partial \mathrm{t}}(\rho \mathrm{h})+\frac{1}{\mathrm{r}}\mathrm{div}(\mathrm{r}\rho\mathbf{u}\mathrm{h})=\frac{1}{\mathrm{r}}\mathrm{div}(\mathrm{rk}\ \mathrm{grad}\,\mathrm{T})+\mathrm{S}_{\mathrm{h}} \tag{5}$$

The form of Eq. (5) enables concentration of all the issues associated with phase change into an energy source term, S_h. Following the expressions derived in [15] and used in FLUENT [14], in the case of isothermal phase change, the source term has the form

$$\mathrm{S}_{\mathrm{h}}=\rho\frac{\partial \Delta \mathrm{H}}{\partial \mathrm{t}} \tag{6}$$

where ΔH is the actual latent heat content in each control volume. The latent heat ΔH is a function of the temperature, i.e.

$$\Delta \mathrm{H}=\mathrm{f}(\mathrm{T}) \tag{7}$$

and may vary between 0 (solid) or L (liquid), the latter being the latent heat of the material. To obtain a solution, the enthalpy-porosity model as implemented in FLUENT iterates between Eqs. (5) and (7). An additional equation is then used to direct ΔH in the

right direction, making the latent heat content ΔH and the temperature T consistent. This equation has the form

$$\Delta H^{n+1} = \Delta H^{n} + \alpha_H c(T - T_f) \tag{8}$$

In FLUENT the under relaxation factor α_H and the number of sweeps, n, of Eq. (8) can be controlled by the user.

In Eqs. (3) and (4), the function A is written as

$$A = -\frac{C(1-\lambda)^2}{(\lambda^3 + q)} \tag{9}$$

where $q=0.001$ is introduced to avoid any division by zero and C is assumed constant and set equal to 1.6×10^3 kg/(m^3 s), as suggested in [15]. The momentum and continuity equations are solved in the entire domain. When the solid fraction in a computational cell approaches the value of 1, Eq. (9) is modelled so that the Au and Av terms dominate all other terms in the momentum equations and the velocity is forced to assume a value close to zero. In the case of isothermal phase change, the transition region is not present. In this case, the melt front should be one cell thick, i.e. the solid fraction should be between 0 and 1 only in a line of single cells representing the position of the melt front [14].

Boundary conditions

A known temperature distribution, uniform along the radial coordinate and variable in time, is assigned as the boundary condition on the top and bottom surfaces:

$$T(r,0,t) = T_c(t), \quad 0 \leq r \leq R, \quad \text{and} \quad t > 0 \tag{10}$$

$$T(r,H,t) = T_h(t), \quad 0 \leq r \leq R, \quad \text{and} \quad t > 0 \tag{11}$$

On the side surface the thermal coupling with the environment is modelled through a boundary condition of the third kind, where the ambient temperature T_e is a function of time:

$$\left[k\frac{\partial T}{\partial r}\right]_{r=R} = U[T_e(t) - T], \quad 0 \leq z \leq H, \quad r = R \quad \text{and} \quad t > 0 \tag{12}$$

The overall heat transfer coefficient U takes into consideration conduction through the polystyrene layer and both convection and radiation heat exchange with the environment.

On the axis of symmetry, a symmetry boundary condition has been considered for all the variables. For the velocity field in the liquid phase, the no-slip condition on all the domain walls has been considered.

Initial conditions

The initial conditions are:

$$T_s(r,z,t=0) = T_i, \quad 0 \leq r \leq R \tag{13}$$

Since the cavity is initially filled with solid *n*-octadecane, at the beginning of the process the velocity is always zero:

$$u(r,z,t=0) = 0, \quad 0 \leq z \leq H, \quad 0 \leq r \leq R \tag{14}$$

$$v(r,z,t=0) = 0, \quad 0 \leq z \leq H, \quad 0 \leq r \leq R \tag{15}$$

Test Cases

The performance of the CFD code in this particular application has been evaluated with two test cases. In the first one, a comparison between the numerical results and the analytical solution of a conduction-dominated freezing in a semi-infinite corner is performed. In the second case, a conduction-convection numerical solution proposed in [15] is compared with the FLUENT solution.

Test Case 1—Conduction-Dominated Phase Change. This test refers to an analytical solution obtained by Rathjen and Jiji [16]. A semi-infinite corner region, $x>0$ and $y>0$, is filled with a liquid initially at a uniform temperature, $T_i=0.3$°C, which is above its freezing point ($T_f=0.0$°C). At time $t=0$, the boundary surfaces at $x=0$ and $y=0$ are lowered down to a temperature below the freezing point, allowing the beginning of the solidification process; hence:

$$T_w(0,y,t) = T_w(x,0,t) = -1.0°C, \quad t \geq 0$$

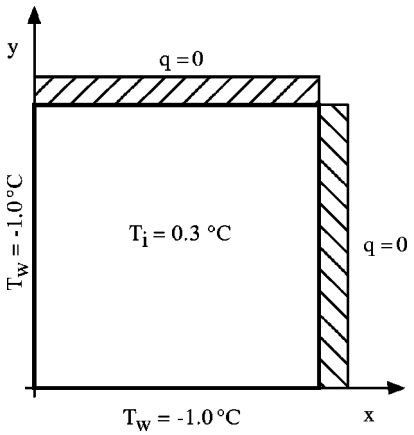

Fig. 2 Test case 1—Problem statement

In Fig. 2, the problem statement is reported. A square corner with side of length L equal to 1 m is used as the computational domain. On the surfaces at $x=1$ m and $y=1$ m, an adiabatic condition is set.

The test is performed adopting the conditions proposed by Gong and Mujumdar [17] to solve the same problem, that is: (i) a 20×20 uniform grid; (ii) a full implicit temporal scheme with a constant time step $\Delta t = 10^{-3}$ s; (iii) thermophysical properties equal for the two phases: $\rho_l=\rho_s=1$ kg/m^3, $k_l=k_s=1$ W/(m °C), $c_l=c_s=1$ J/(kg °C) and $L=0.25$ J/kg. The Stefan number Ste, representing the latent to sensible heat ratio, is usually considered a significant parameter to describe the operating condition of a system undergoing phase change, since this number governs the temperature gradient discontinuity at the interface. In the literature, it is usually considered that the higher the Stefan number, the more difficult the numerical solution of a phase change problem. In this case, since an enthalpy method is used, the problem Stefan number, $Ste=1.2$, can be considered quite critical [18].

In Fig. 3, a comparison between analytical and numerical results for the non-dimensional interface position is reported. As can be seen, the agreement is very convincing.

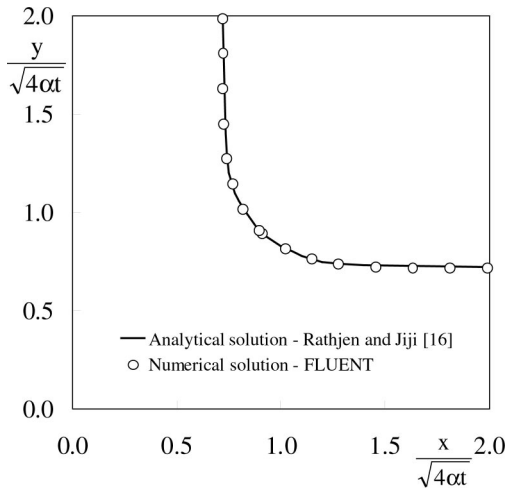

Fig. 3 Test case 1—Comparison between analytical and numerical results of the interface position

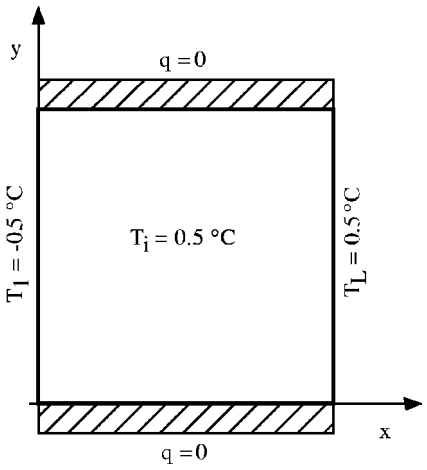

Fig. 4 Test case 2—Problem statement

At t=0, the sudden change in the boundary conditions did not originate significant convergence difficulty. In this case, the solution converged quite easily in a few inner iterations. Going further in time, to obtain a satisfactory accuracy of the interface displacement, the under relaxation factor α_H in Eq. (8) had to be set to quite a small value ($\alpha_H=0.1$) with a corresponding increase of the sweeps number.

Test Case 2—Conduction-Convection Phase Change. The second test refers to the numerical solution of a conduction-convection problem proposed by Voeller and Prakash [15]. A square cavity (side length L=1 m) is filled with a liquid initially at $T_i=0.5°C$. At t=0, the boundary surface x=0 is lowered down to the temperature $T_l=-0.5°C$, below its freezing temperature, $T_f=0.0°C$. The boundary surface at x=L is kept at a constant temperature, $T_L=0.5°C$. The upper (y=L) and lower (y=0) boundary surface are adiabatic. The thermophysical properties are as follows: $\rho_l=\rho_s=1$ kg/m^3, $k_l=k_s=0.001$ W/(m°C), $c_l=c_s=1$ J/(kg°C), L=5 J/kg, $\mu=1$ Pa s, $\beta=0.01°C^{-1}$, g=1000 m/s^2. The Stefan number is equal to 10. In Fig. 4 the problem statement is reported.

This test case was solved in [15] with different grids and test conditions. In this paper, for comparison, the case in which the solidification temperature (solidus) and the melting temperature (liquidus) are different and equal to −0.1°C and +0.1°C, respectively, is simulated. The calculation is performed adopting the same conditions used in [15]. In particular, a 40×40 computational grid is used and the final time t=1000 s is reached. As in [15], initially a fixed time step Δt=10 s is used.

In the present study, for the discretisation of the convective term the QUICK difference scheme is used; for the pressure-velocity coupling the SIMPLE algorithm is used.

Using the above conditions, the calculations with FLUENT did not converge. This was probably due to the abrupt change at time t=0 in the boundary condition at x=0. At this time, in fact, the melting temperature is instantaneously reached and the first melted layer should appear inside the domain. This situation is handled with difficulty by the code. So, to obtain a solution, a different approach was adopted. In particular, three steps were defined:

Step 1. The momentum equations are excluded from the calculation. In this manner, a conduction-dominated solution is obtained and used as the starting solution for the subsequent calculation including convection. Convergence is quite easily reached.

Step 2. The solution of the momentum equations is included. In the first part of the calculation, variable time steps and Under Relaxation Factors (URFs) are adopted. Initially, the time step and the URFs are both initially set to a very small value (Δt=0.01 s; URF_1 as in Table 1). In addition, the gravitational acceleration is set to 1 m/s^2. In this manner, performing a number of time iterations coupled to a high number of inner iteration sweeps, the flow field is initialised with good convergence rate and accuracy.

Table 1 URFs for test case 2

Equation		URF_1	URF_2
Momentum	$\alpha_{u,v}$	0.1	0.7
Mass	α_p	0.2	0.8
Energy	α_h	0.5	0.8
Latent Heat	α_H	0.1	0.5

Step 3. The gravitational acceleration is set to the requested value (g=1000 m/s^2). The time step is progressively increased until it reaches the chosen value, Δt=10 s. At this point, the inner iterations are set to a lower value, but enough to assure a good convergence, and the URFs, reported as URF_2 in Table 1, are increased.

The position of the interface and the velocity vectors obtained using FLUENT are shown in Fig. 5. The final results are in good agreement with the corresponding results presented in [15] and in [18].

Results and Discussion

As a final example of application, the experiment on the cylinder cavity, described extensively in [19], was simulated numerically. The temperature data, obtained by means of six thermocouples placed inside the specimen at a radius r=0.016 m and gathered every 10 minutes, are available. The estimated uncertainty on the temperature data was ±0.15°C. In this experiment, the top and bottom surfaces were maintained below the melting temperature for about 30 minutes before switching on the heater; after this time, the sudden increase of the heat flux quickly raised the top surface temperature and the melting process began.

In the numerical simulation, the top and bottom measured temperature values were imposed as boundary conditions. A linear interpolation of the sample data was used to calculate the boundary values needed in the computation but not available experimentally. The thermal coupling between cylinder and environment was taken into account through an overall heat transfer coefficient equal to 0.5 W/(m^2 °C). The external temperature, recorded every two hours, was considered variable in the model and taken into account through a step-wise temperature-time function.

The PCM used in the experiment is 99% pure *n*-octadecane ($C_{18}H_{38}$). The properties proposed by Chung et al. [20] listed in Table 2 were used. As can be seen, all the thermophysical properties except the density are considered constant with temperature

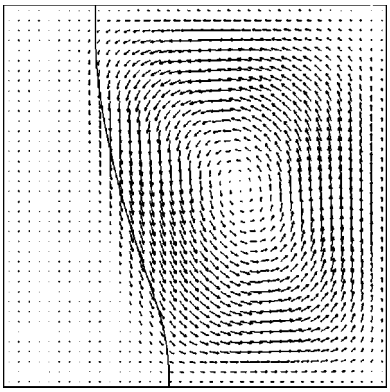

Fig. 5 Test case 2—Isotherm at T=0°C (interface position) and velocity field at t=1000 s

Table 2 Thermophysical properties of *n*-octadecane

Properties	Value		Ref.
Liquid density ρ_1	814	kg/m^3	
Solid density ρ_s	814	kg/m^3	
Liquid conductivity λ_1	0.157	W/(m°C)	
Solid conductivity λ_s	0.390	W/(m°C)	
Liquid specific heat c_1	2200	J/(kg°C)	[20]
Solid specific heat c_s	1900	J/(kg°C)	
Latent heat L	241360	J/kg	
Viscosity μ	3.878×10^{-3}	Pa s	
Thermal expansion coefficient β	9.1×10^{-4}	°C^{-1}	
Melting temperature T_f	27.5	°C	[19]

Table 3 URFs and time steps for the experiment simulation

	Δt	$\alpha_{u,v}$	α_p	α_h	α_H
0<t≤2400 s	5 s	···	···	0.8	···
2400 s<t≤4800 s	0.5 s	···	···	0.7	0.1
4800 s<t≤4801 s	0.01s	0.02	0.1	0.5	0.01
4801 s<t≤4805 s	0.05s	0.2	0.3	0.7	0.05
4805 s<t≤4808 s	0.1 s	0.5	0.3	0.8	0.05
4808 s<t≤4810 s	0.2 s	0.5	0.5	0.8	0.05
t>4810 s	0.5 s	0.5	0.5	0.8	0.05

and phase dependent. The melting temperature value was chosen in accordance with Casano [19], who measured this value during his experiment.

The method of handling the phase change implemented in the code cannot account directly for different properties in the two phases. Thus, the specific heat and the thermal conductivity were fictitiously treated as temperature dependent. If a property-temperature relationship with a sharp step at the melting temperature is used, the calculation diverges. For this reason, ramp-shaped (T,k) and (T,c) functions were used to simulate the solid-liquid transition. The minimum interval of the ramp temperature ΔT_{AB}, allowing a convergent solution, resulted equal to 1.08°C for the thermal conductivity and equal to 1.06°C for the specific heat. The two temperature-property functions are shown in Fig. 6.

Grid-dependence experiments suggested the choice of a 64×64 elements computational grid, uniformly distributed in radial and axial direction, considering both accuracy and computational time as decisional parameters.

To achieve good convergence and accuracy, a computational strategy was developed. In particular, the appearance of the first melted layer is handled with difficulty by FLUENT, and, thus, a procedure similar to test case 2 was adopted. Hence, these steps were followed:

1. During the first period (0÷2400 s) the whole domain remains under the melting temperature (T_f=27.5°C), and thus, the process is only conductive. Hence, at the beginning of the numerical simulation, the momentum equations were turned off for the first 2400 s. In this manner, only the energy equation is solved and the convergence is easily reached. A time step Δt=5 s was used with good accuracy.
2. When t>2400 s, on the top surface the melting temperature is exceeded. The subsequent time iterations were still executed by considering the problem conduction-dominated. In fact, the phase change process has to be initialised and a thin layer of liquid phase has to be distinguishable inside the domain in order to obtain convergence when the momentum equations are included. This layer of liquid phase should be at least two cells thick. Thus, the conduction-based simulation was carried out until the time t=4800 s was reached. To obtain the convergence, the time step was set to Δt=0.5 s, while α_H was set equal to 0.1.
3. For t>4800 s, the momentum equations were finally included. For the first 10 s (4800 s<t≤4810 s), the following strategy was adopted: (i) initially, some time iterations were performed with a small time step and small URFs (see Table 3) to initialize the flow field inside the liquid layer. To obtain good accuracy, a total amount of 200 inner sweeps were set for each time step; (ii) then, the time step and the URFs were increased, the former up to a final value of 0.5 and the latter up to the values reported in Table 3. The inner sweeps were then lowered to 50.
4. For t>4810 s, the values of the time step, URFs and inner sweeps were kept constant for the remainder of the simulation.

Comments to Numerical and Experimental Results. In Fig. 7, three temperature distributions are compared: (i) the data measured during the experiment (the experimental uncertainty ±0.15°C is represented by the symbol size), (ii) the results obtained with FLUENT, and (iii) the results obtained through an implicit conduction-based two-dimensional code [13]. This code uses a modified conventional method, with a front tracking algorithm for the interface advancement; these calculations were performed on a 31×241 uniform grid and with a fixed time step Δt=60 s.

In Fig. 7, the presence of two phases separated by an interface at a well-defined temperature is clearly readable. Furthermore, it is possible to notice that the temperature increases very slowly inside the solid phase, while the increase is faster when the PCM is liquid. This occurs because most of the thermal flux released by

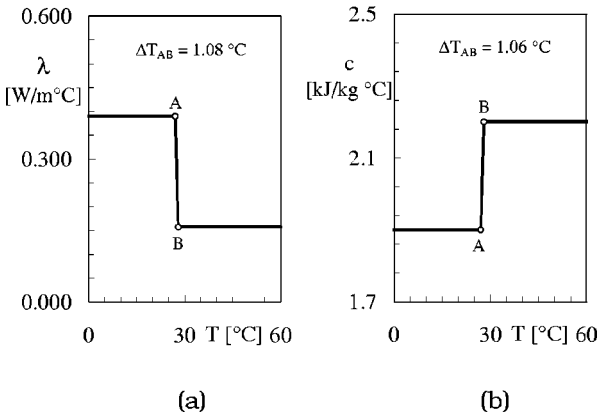

Fig. 6 Property-temperature functions: (a) thermal conductivity; (b) specific heat

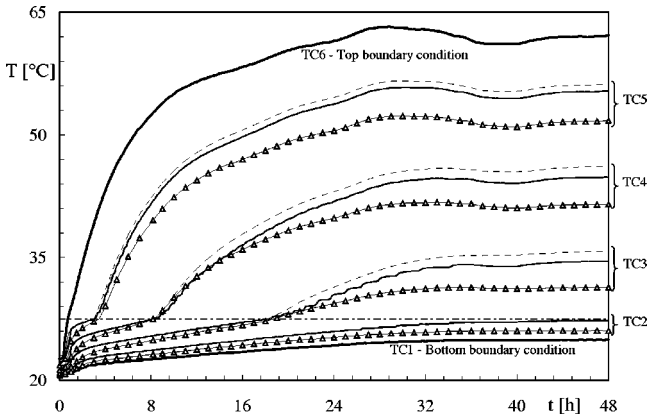

Fig. 7 Experimental and numerical temperature distributions: (—) experimental and numerical boundary conditions, (△) experimental data, (——) FLUENT numerical results, (---) Pinelli et al. [13] numerical results, (—·—) melting temperature T_f.

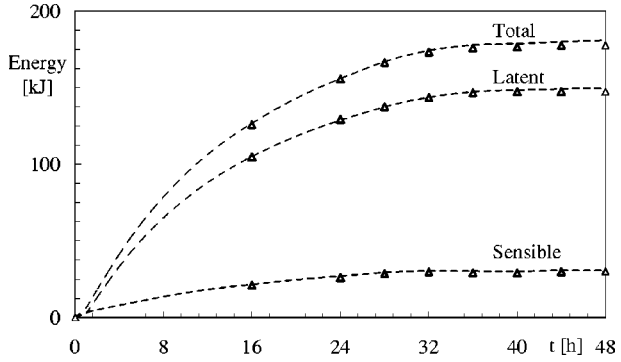

Fig. 8 Calculated energy storage: (△) FLUENT numerical results, (---) Pinelli et al. [13] numerical results

the heater and entering the system is used for the melting and the interface advancement; only a small amount of the flux is available for the heating of the solid phase. Qualitatively, both the simulations (with and without flow motion) show temperature distributions in good agreement with the experimental data. Quantitatively, the taking into account of natural convection produces a significant improvement in the agreement between numerical results and experimental data. The maximum difference is approximately 4.5°C in the conduction-based simulation, while in the conduction-convection simulation this difference is lowered down to 3.5°C. Thus, the natural convection significantly affects the heat exchange and its neglect can originate differences between numerical and experimental results.

In Fig. 7 it is also possible to notice the wiggle-shaped form of the temperature distributions obtained with FLUENT, particularly for thermocouple 3 and 4. This behavior is due to the enthalpy methods used in the code. In fact, the interface position is not tracked explicitly, as for the front tracking conventional method, but determined indirectly from the liquid fraction. It is also noticeable, even if hardly appreciable, that in the numerical simulation the interface advances faster than in the experiment.

In Fig. 8, the calculated energy storage is shown. With respect to the conduction-based simulation, the presence of natural convection reduces, even if weakly, the total energy stored, which reaches a final value equal to 171 kJ. This can be attributed to the increased thermal coupling with the environment produced by the fluid circulation inside the liquid phase. Quantitatively, the greatest difference between the two cases is in the calculated sensible energy storage, which gives, in this problem characterized by quite a high Stefan number (Ste=0.32), a significant contribution to the total energy storage.

The numerical simulations also give interesting information on the fluid flow of the melted layer. In Fig. 9, the flow field at four different times (t=16 h, 24 h, 36 h and 48 h) is reported, together with the melting temperature isotherm T_f. This fluid flow is originated by the temperature difference between the core of the domain and the cylinder side surface, due to the coupling with the environment.

A major circulation is present near the upper corner of the cavity, in correspondence with the highest values of the flow field velocity. At the four times shown in the Fig. 9 this circulation is always present and the liquid/solid separation surface seems to be almost flat. Furthermore, it is possible to notice that the interface advancement is fast in the first 24 h (Figs. 9a and 9b), while in the last 12 h (Figs. 9c and 9d) the advancement slows down due to the asymptotic attainment of a steady state condition. It is also possible to notice that, at t=16 h (Fig. 9a), the convection cells which were present earlier (they are noticeable at t=10 h, Fig. 10) have almost vanished and the major circulation located on the upper corner is dominant.

In Fig. 10, the flow field at t=10 h is reported in detail. As can

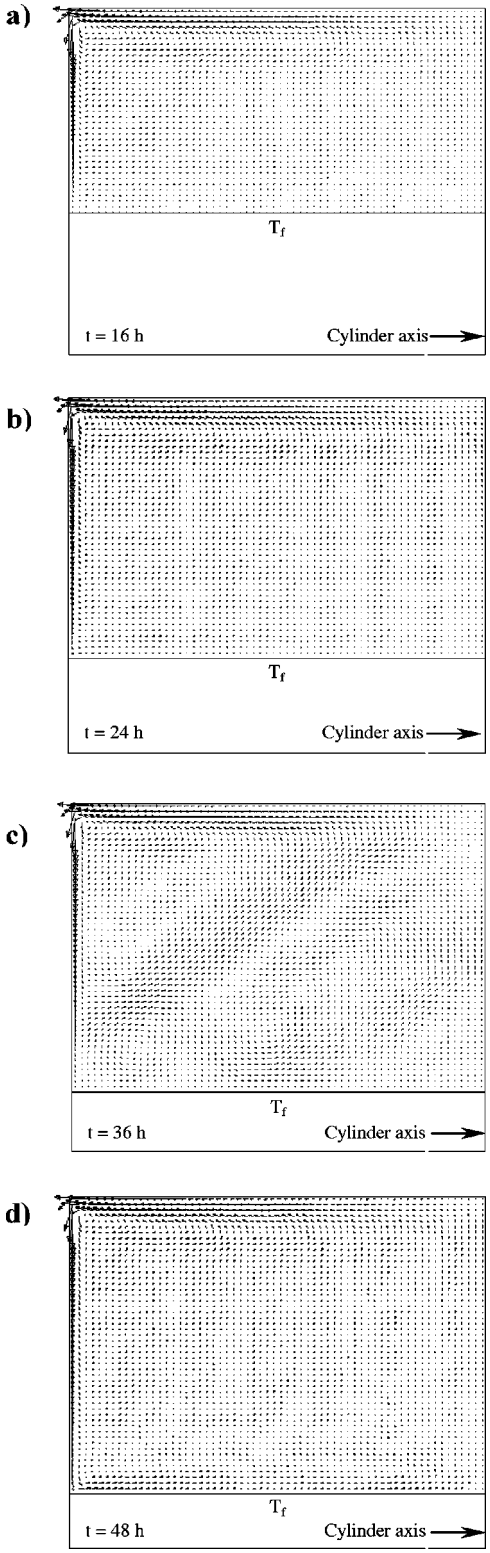

Fig. 9 Flow field and melting temperature isotherm T_f at times t=16 h, 24 h, 36 h and 48 h

be seen, the presence of three convection cells, which occupy the entire liquid region, is recognisable. It can be noticed that the length of scale of the convection cells is of the same size as the melted layer thickness. The morphology of these convection cells seems to be in qualitative agreement with the results obtained in similar conditions by other authors, both numerically and experimentally [11,21–23].

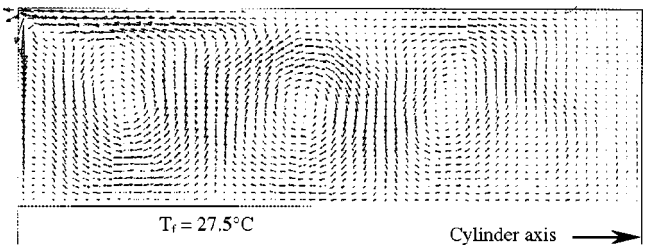

Fig. 10 Flow field and melting temperature isotherm T_f at time t=10 h

Sources of Discrepancy Between Numerical and Experimental Results. The analysis showed that, even if natural circulation in the liquid phase is considered, numerical results still remain quite far from experimental data. The reason of this discrepancy can be due to:

1. the uncertainty on the *n*-octadecane thermophysical properties values. Although in literature the properties of this material are considered well-established, significant discrepancies among the value proposed by different authors were found, in particular for the thermal conductivity and for the solid phase density [24]. Furthermore, published works often reported the values of the properties in an incomplete and/or non-dimensional form. Puyado et al. [25] were among the first authors which reported explicitly the property values as a function of temperature. Other values which have been extensively used by many authors are that suggested by Humpries and Grigg [3]. Chung et al. [20] recently proposed one of the most complete set of property values. Comparing the values of all the *n*-octadecane thermophysical properties founded in the open literature and reported extensively in [24], it was possible to notice that:
   a) there is a remarkable spread of the solid phase density value;
   b) in the past, the value of the solid thermal conductivity was considered equal to that of the liquid phase and temperature dependent [25]; at the contrary, recently a value constant with temperature and equal to more than twice that of the liquid phase value was considered [20]. This leads to consider that the value of a key parameter such as the thermal conductivity solid/liquid ratio can assume a value included in a very wide range, namely from 1 to more than 2. In the paper, the values of the *n*-octadecane thermophysical properties proposed by Chung et al. [20] are used, since: (i) using these properties, in [20] a very good agreement between numerical results and experimental data of Ho and Viskanta [26] was found and (ii) the value of the thermal conductivity solid/liquid ratio is 2.5, in agreement with the tendency shown in the open literature in recent years.
2. The presence of the polycarbonate hollow cylinder in which the PCM is confined. The polycarbonate was chosen in order to have walls with a thermal conductivity very similar to the conductivity of the PCM. This was done in order to have a similar thermal behavior along the vertical test chamber walls and in the specimen. However, recent analyses [27], based on the suggestion proposed by Hale and Viskanta [10] about the role played by the coupling between lateral solid walls and PCM it self, show that also when the thermal conductivity of the walls and of the PCM are the same, the different phenomena occurring in the PCM (discontinuous temperature profile due to phase change) and in the walls (pure conduction) significantly modify the temperature distribution within the specimen, particularly near the walls.
3. A refined evaluation of the coupling with the environment. In fact, the uncertainty on assessing the value of the convective heat transfer coefficient is still quite high. However, this effect seems to be less significant with respect to the two ones outlined above.
4. The neglecting of the thermal radiation within the media, that is the PCM is considered opaque. Nearly all the studies on energy storage using paraffin as PCMs do not take into account this contribution to heat transfer, and, in the few cases in which radiation is considered, the problem is solved neglecting the natural convection in the liquid phase [28]. Nevertheless, some authors suggests that internal radiant transfer could have a significant effect for accurately predicting temperature distributions, interface position and energy fluxes [29]. In this paper, the contribution of this effect seems to be negligible. In fact, the highest temperature reached by the heater is about 63°C. At this temperature, the radiant emission is almost completely in the near-infrared part of the spectrum. In this region, the spectral absorption coefficient of the *n*-octadecane is very high [30] and, thus, most of the radiation is absorbed by the PCM at or near the upper surface of the specimen. Consequently, once the melting is began and the liquid layer progressively thickens, the solid/liquid separation surface is no longer reached by the radiative flux from the heater.

Future works will regard a sensitivity analysis on the thermophysical properties of the *n*-octadecane and the numerical simulation of the conjugate heat transfer at the lateral boundary of the specimen originated by the presence of the polycarbonate solid walls.

Concluding Remarks

A cylinder cavity heated from above and filled with a PCM, used as an energy storage device, has been studied. The natural circulation originated in the liquid phase and due to the thermal coupling with the environment was suspected of affecting the heat transfer process during an experiment conducted on the device. To study numerically this problem, the commercial CFD code FLUENT, which uses a control volume finite-difference and the enthalpy-porosity method for the phase-change interface advancement, was used. A general-purpose code like FLUENT, when applied to this difficult case, can offer many opportunities, because it easily takes into account 3D geometry and flow field motion. On the contrary, further problems are introduced, because the code used is well tailored to solve only some particular phase change problems, for example the solidification of metal ingots. For this reason a methodological analysis on the performances of the code must be carried out before its utilisation for the specific problem. In the paper, a procedure has been set up, allowing convergent and accurate solutions. The procedure consists of a numerical strategy in order to face and solve the main problems encountered during the simulations, such as the different values of the properties in the liquid and solid phase, the phase change process initialization and the variable-in-time boundary conditions. The results obtained from the simulation of the experiment showed that effectively the natural circulation is present, even if the thermal coupling with the ambient is small, and affects the heat transfer process. The analysis also showed how accounting for natural convection in the melted PCM, when comparing the results of the commercial CFD code with the conduction-based solutions, produces a significant quantitative improvement in the agreement between numerical results and experimental data.

Acknowledgments

Financial support for this work was furnished by MURST 60%. The authors gratefully acknowledge Dr. G. Casano for his helpful suggestions.

Nomenclature

A = porosity function for the momentum equation [kg/(m^3 s)]
c = specific heat [J/(kg °C)]
C = porosity constant [kg/(m^3 s)]
g = gravitational acceleration [m/s^2]
h = specific enthalpy [J/kg]
H = cylinder height [m]
k = thermal conductivity [W/(m °C)]
L = latent heat of fusion [J/kg] or length [m]
p = pressure [Pa]
R = cylinder radius [m]
r = radial co–ordinate [m]
S_h = energy source term [W/m^3]
Ste = $=c_s(T_f-T_f)/L$, Stefan number [−]
t = time [s]
T = temperature [°C]
u = velocity vector [m/s]
u = r-direction velocity [m/s]
U = overall heat transfer coefficient [W/(m^2 °C)]
v = z-direction velocity [m/s]
z = axial co-ordinate [m]
α = under relaxation factor [−]
β = thermal expansion coefficient [°C^{-1}]
λ = porosity [−]
μ = molecular viscosity [Pa s]
ρ = density [kg/m^3]
ΔH = actual latent heat content [J/kg]

Subscripts

AB = ramp interval
c = cold
e = environment
f = melting
h = hot or referred to energy equation
H = referred to actual latent heat content
i = initial
l = liquid or left lateral surface
L = right lateral surface
p = referred to mass equation
ref = reference condition
s = solid
w = wall
u = referred to radial momentum equation
v = referred to axial momentum equation

Superscripts

n = *n*-th sweep

Acronyms

CFD = Computational Fluid Dynamic
PCM = Phase Change Material
TC = ThermoCouple
URF = Under Relaxation Factor

References

[1] Brown, D. R., Katipamula, S., and Koneynbelt, J. H., 1996, ''A Comparative Assessment of Alternative Combustion Turbine Inlet Cooling Systems,'' Technical Report No. 10966 (under DOE contract No. DE-AC06-76RLO 1830), PNNL, Washington, DC.
[2] Pilavachi, P. A., 2000, ''Power Generation With Gas Turbine Systems and Combined Heat and Power,'' Appl. Therm. Eng., **20**, pp. 1421–1429.
[3] Humpries, W. R., and Griggs, E. I., 1977, ''A Design Handbook for Phase Change Thermal Control and Energy Storage Devices,'' Technical Paper No. 1074, NASA, Washington, DC.
[4] Bellecci, C., and Conti, M., 1993, ''Latent Heat Thermal Storage for Solar Dynamic Power Generation,'' Sol. Energy, **51**, pp. 169–173.
[5] Carlsaw, H. S., and Jaeger, J. C., 1959, Conduction of Heat in Solids, Clarendon Press, Oxford.
[6] Muehlbauer, J. C., and Sunderland, J. E., 1965, ''Heat Conduction With Freezing or Melting,'' Appl. Mech. Rev., **18**, pp. 951–959.
[7] Fukusako, S., and Seki, N., 1987, ''Fundamental Aspects of Analytical and Numerical Methods on Freezing and Melting Heat-Transfer Problems,'' Annual Review of Numerical Fluid Mechanics and Heat Transfer, T. C. Chawla, eds., Hemisphere, Washington, DC, **1**, pp. 351–402.
[8] Yao, L. S., and Prusa, J., 1989, ''Melting and Freezing,'' Adv. Heat Transfer, **19**, pp. 1–95.
[9] Voller, V. R., Swaminathan, C. R., and Thomas, B. G., 1990, ''Fixed Grid Techniques for Phase Change Problems: A Review,'' Int. J. Numer. Methods Eng., **30**, pp. 875–898.
[10] Hale, N. W., and Viskanta, R., 1980, ''Solid-Liquid Phase-Change Heat Transfer and Interface Motion in Materials Cooled or Heated From Above or Below,'' Int. J. Heat Mass Transfer, **23**, pp. 283–292.
[11] Hernandez-Guerrero, A., Aceves, S., Cabrera-Ruiz, E., and Baltazar-Cervantes, J. C., 1999, ''Modeling of the Charge and Discharge Processes in Energy Storage Cells,'' En. Conv., **40**, pp. 1753–1763.
[12] Casano, G., Piva, S., and Pagliarini, G., 1997, ''Theoretical and Experimental Investigation on the Thermal Energy Storage in Phase Change Systems (in Italian),'' Proc. XV Congresso Nazionale UIT, ETS, Pisa, **1**, pp. 509–520.
[13] Pinelli, M., Casano, G., and Piva, S., 2000, ''Solid-liquid Phase-Change Heat Transfer in a Vertical Cylinder Heated From Above,'' Int. J. Heat and Technology, **18**, pp. 61–67.
[14] Fluent Incorporated, Centerra Resource Park, 10 Cavendish Court, Lebanon, FLUENT User's Guide, Rel. 4.48.
[15] Voller, V. R., and Prakash, C., 1987, ''A Fixed Grid Numerical Modelling Methodology for Convection-Diffusion Mushy Region Phase-Change Problems,'' Int. J. Heat Mass Transfer, **30**, pp. 1709–1719.
[16] Rathjen, K. A., and Jiji, M. L., 1971, ''Heat Conduction With Melting or Freezing in a Corner,'' ASME J. Heat Transfer, **93**, pp. 101–109.
[17] Gong, Z. X., and Mujumdar, A. S., 1997, ''Non-convergence Versus Non-Conservation in Effective Heat Capacity Method for Phase Change Problems,'' Int. J. Numer. Methods Heat Fluid Flow, **7**, pp. 565–579.
[18] Nigro, N., Huespe, A., and Fachinotti, V., 2000, ''Phasewise Numerical Integration of Finite Element Method Applied to Solidification Processes,'' Int. J. Heat Mass Transfer, **43**, pp. 1053–1066.
[19] Casano, G., 1996, ''Theoretical and Experimental Investigation on the Thermal Energy Storage in Phase Change Systems (in Italian),'' Ph.D. Thesis, University of Bologna, Bologna.
[20] Chung, J. D., Lee, J. S., and Yoo, H., 1997, ''Thermal Instability During the Melting Process in an Isothermally Heated Horizontal Cylinder,'' Int. J. Heat Mass Transfer, **40**, pp. 3899–3907.
[21] Gong, Z. X., and Mujumdar, A. S., 1998, ''Flow and Heat Transfer in Convection-Dominated Melting in a Rectangular Cavity Heated From Below,'' Int. J. Heat Mass Transfer, **41**, pp. 2573–2580.
[22] Gau, C., and Viskanta, R., 1983, ''Flow Visualisation During Solid-Liquid Phase Change Heat Transfer I. Freezing in a Rectangular Cavity,'' Int. Commun. Heat Mass Transfer, **10**, pp. 173–181.
[23] Diaz, L. A., and Viskanta, R., 1984, ''Visualization of the Solid-Liquid Interface Morphology Formed by Natural Convection During Melting of a Solid From Below,'' Int. Commun. Heat Mass Transfer, **11**, pp. 35–43.
[24] Pinelli, M., 2001, ''Numerical Investigation of Systems With Solid-Liquid Phase Change for Energy Storage (in Italian),'' Ph.D. Thesis, University of Bologna, Bologna.
[25] Puyado, P. R., Stermole, F. J., and Golden, J. O., 1969, ''Melting of Finite Paraffin Slab as Applied to Phase-Change Thermal Control,'' J. Spacecr. Rockets, **6**, pp. 280–284.
[26] Ho, C. J., and Viskanta, R., 1984, ''Heat Transfer During Inward Melting in a Horizontal Tube,'' Int. J. Heat Mass Transfer, **27**, pp. 705–716.
[27] Casano, G., and Piva, S., 2003, ''Solid-liquid Phase Change Heat Transfer: Numerical Investigation of the Wall Construction in the Test Cell,'' Proc. Seminar EUROTHERM 69 Heat and Mass Transfer in Solid-liquid Phase Change Processes, B. Sarler and D. Gobin, eds., Ljubljana, Slovenia, pp. 117–225.
[28] Abrams, M., and Viskanta, R., 1974, ''The Effect of Radiation Heat Transfer Upon the Melting and Solidification of Semitransparent Crystals,'' J. Heat Transfer, **96**, pp. 184–196.
[29] Yimer, B., 1996, ''Thermal Radiation Effects in Phase-Change Energy-Storage Systems,'' Energy, **21**, pp. 1277–1286.
[30] Diaz, L. A., and Viskanta, R., 1986, ''Experiments and Analysis on the Melting of a Semitransparent Material by Radiation,'' Wärme-und Stoffübertragung, **20**, pp. 311–321.

Stefano Piva Full Professor of Thermodynamics and Heat and Mass Transfer at the University of Ferrara. Since November 2001 he is Head of the Dipartimento di Ingegneria of the same University. He is author or co-author of more than 60 papers presented at Italian or international conferences and published on Italian or international technical journals. His principal interest has been in heat transfer, applied thermodynamics and thermal plant design.

Michele Pinelli Assistant Professor of Energy Systems at the University of Ferrara. He graduated in Mechanical Engineering at the University of Bologna, where he also received his Ph.D. (2001). His research activity focuses on energy systems analysis, gas turbine health monitoring techniques, computational heat transfer and fluid flow, with special interest in turbomachinery and combustion process application.